

ELECTRICITY AND FRESHWATER MACRO-PROJECT IN THE ARID AFRICAN LANDSCAPE OF DJIBOUTI

Radu D. Rugescu

Richard B. Cathcart

Dragos Ronald Rugescu

Sergiu Paul Vataman

INTRODUCTION

Bordering the Gulf of Aden and the Red Sea, the economically underdeveloped Republic of Djibouti gained its independence on June 27, 1977 from the former territory of the French Somaliland (later called the French Territory of the Afars and Issas), which was created in the first half of the 19th Century as a result of French interest in the Horn of Africa. It is a 23,200 km² coastal dryland ecosystem-nation without any perennial rivers, generally described as a drab and hot desert-type landscape of ochre-colored geomorphology situated near the Bab-al-Mandab Strait, international shipping's southernmost Red Sea entrance/exit (Fig. 1).



Figure 1: Map of the Republic of Djibouti indicating its most pronounced physical features as well as its immediate surroundings.

A Bab-al-Mandab dam-construction macro-project has been proposed to regulate the Red Sea for the purpose of electricity generation on a truly monumental scale (Schuiling et al 2007); were the Bab-al-Mandab Dam built it might induce further seaport development in Djibouti. Macro-engineers have already proposed a plan to “tent” most of the Sahara, which lies to the west of Djibouti (Cathcart and Badescu, 2004).

The DESERTEC Foundation is actively formulating a macro-engineering concept to produce electricity and freshwater on a spatially semi-continental scale (Strahan, 2009). During 2010, DESERTEC's geographical planning boundaries, encompassing spatially widespread industrial-scale electricity generation installations (concentrating solar power, photovoltaics, wind-power, geothermal, biomass and hydropower), do not yet include any Republic of Djibouti territory. Djibouti has an estimated mid-2010 human population of fewer than one million citizens (~750,000 persons).

Most of land-locked Ethiopia's imports and exports pass through Djibouti's well-developed seaports, so improvement of road, railway and ocean-shipping access should be very helpful with the future economical and social progress of several other inland East Africa countries. The Republic of Djibouti and Ethiopia share a 337 km border (Mugnier, 2008). Ethiopia is among the most recent of states to become land-locked and is trying to cope successfully with its dependency on coastal Djibouti; its external trade stability will, thus, be tied to the crucial infrastructure and vital economic prosperity of the littoral state of Djibouti. (By 2007, Djibouti's domestic electricity supplier, Electricite de Djibouti, had entered into an agreement with the Ethiopian Electric Power Corporation to share any power surplus that either country may develop.) The metric-gauge (1,000 mm) railway

Chemin de Fer Djibouti-Ethiopian (CDE) connects the Port of Djibouti with Dire Dawe, Ethiopia. Djibouti's coastline length is 314 km. DESERTEC's service region expansion could foster a spin-off regional development, a Republic of Djibouti macro-project we have dubbed the "Lac Assal Freshwater Distillatory and Energy District" (LAFDED), technically detailed herein. The CDE strategically terminates at the Port of Djibouti and is likely to serve the hinterland of East Africa, perhaps as a regional multi-modal transport hub. Djibouti endures a domestic freshwater shortage, which curtails its progress as a sustainable ecosystem-nation; its arable land is but 0.25% of that ecosystem-nation's territory. The offered LAFDED macro-project is meant to readily, comprehensively, and permanently remedy this unfortunate circumstance of a pervasive civilian potable water limitation and to produce low-cost electrical power.

The oval-shaped Lac Assal (located at $11^{\circ} 28'$ to $11^{\circ} 23'$ North latitude by $42^{\circ} 23'$ to $42^{\circ} 28'$ East longitude), at a negative global sea-level elevation of minus 155 m, is the lowest and geologically the youngest dry-land place on the continent of Africa and is also Africa's most saline lake. Its easternmost shoreline lies ~11-12 km from the Gulf of Aden, separated by a strip of faulted volcanic land ~5 km wide by 12 km long with a maximum above sea-level topographic elevation of ~98 m. Lac Assal proper, consisting of syrup-like brine volume—nearly ten times more concentrated than the nearby Gulf of Aden seawater—amounting to $\sim 420 \times 10^6 \text{ m}^3$, is approximately 54 km^2 in area and is faced by a vast white-colored crystallized sea salt plain (a flat terrain of 60 km^2) on its northern shoreline. The salt pan is quarried commercially, with sea-salt production at Lac Assal started on a semi-industrial scale in 1998. On average, the brine in Lac Assal is $\sim 300 \text{ g/l}$ of sodium chloride (NaCl), with another 100 g/L of various other salts (Brisou et al 1974). Derived mostly from hot springs, the lake's high temperature brine, $33\text{-}34^{\circ} \text{C}$, has a surface density of ~ 1.204 . The mean annual air temperature in this tectonically closed, below world sea-level, basin is a torrid $\sim 33^{\circ} \text{C}$ with maximum monthly means of nearly 40°C in June and July. The mean annual rainfall is $< 200 \text{ mm}$. In other words, per year, freshwater evaporation from Lac Assal must be in the range of $\sim 250\text{-}290 \times 10^6 \text{ m}^3$ (Gasse and Fontes, 1989). The maximum wind, $\sim 14\text{-}15 \text{ m/second}$, impinging Lac Assal is onshore (easterly) 66% of the time and offshore (westerly) 23% of the time; the onshore wind carries more water vapor than the offshore wind over Lac Assal.

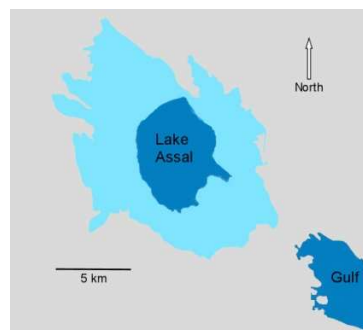


Figure 2: A speculative chart of Lac Assal converted to anthropogenic gulf filled to the current local level of the nearby ocean. Connecting 12 km-long filling canal is not drawn.

Filled to today's global sea-level, the volcano-tectonic crater-basin of Lac Assal, shaped like an ellipse, would be a 340 km^2 body of evaporating seawater amounting to, probably, $< 50 \text{ km}^3$ (Fig. 2). However, in that unique connected state, its usefulness would likely be restricted to simply functioning as an anthropogenic ocean gulf, perhaps a new commercial and naval harbor with a maximum navigational depth in excess of 150 m and a controllable, but unlocked, seawater canal shipping access route. Since the sill between the Ghoubbat-al-Kharab Strait (Fig. 3), situated immediately to the east of the 12 km-long land barrier that isolates the existing Lac Assal, and the Gulf of Aden lies at 4.5 m below extant sea-level, then any large-scale harbor development would necessitate dredging of a harbor approach channel leading to the man-made gulf's proposed canal. Most large 21st Century ships require 40 m of nautical depth to maneuver safely. So, the proposed canal, measuring 12 km long by 100 m wide with a navigational depth of 40 might necessitate the removal of $> 192,000,000 \text{ m}^3$ of material ($> 0.192 \text{ km}^3$) which can be done economically, we think, by nuclear-powered dredgers (Cathcart, 2008).



Figure 3. Lac Assal, fringed on the northwest by a massive arid terrain of air-exposed sea-salt, is separated from the Gulf of Tadjoura (bottom right), by a 5 km-wide volcanic land form known as the Ghoubbat-al-Kharab (“navel of the world”). Satellite image.

There is a network of some 30 GPS sites established in the Republic of Djibouti to monitor the Lac Assal-Ghoubbet Rift System (Vigny et al, 2007) which seems to be widening at a current measured yearly rate of ~16 mm; Djibouti endures the focused devastation of earthquakes—extensional faults accommodate 5-15% of the total extension of the Lac Assal Rift. It is widely assumed that, in a million years possibly, a geological rift will permit the ocean to flood the low-lying Lac Assal Basin with seawater (Backer et al 1973). Sub-aerial geological rift zones in Iceland—where volcanic eruptions of airborne ash, starting in 2010, interfered with scheduled transatlantic air traffic—and in Djibouti afford geoscientists glimpses of dyke injections at Earth’s divergent plate tectonic boundaries. The two month-long 1978 Lac Assal-Ghoubbet Rift event-process commenced with a 5.3 Richter Scale temblor near the “...center of a 60 km-long segment followed by a week-long volcanic eruption...” (Rowland et al 2007). Deep-drilling, at least six wells completed so far (Asal 1-6), has been conducted in Djibouti on the landform named Ghoubbet-al-Kharab that separates Lac Assal from a gulf facing the Indian Ocean and a technical study, financed by The World Bank Group as Project P000612 for USD 9.2 million related to the feasibility of a 30 MW power-plant at Assal was completed by 1992. The estimated installation cost of the power-plant was USD 117 million. Since the GDP of the Republic of Djibouti is only about one billion US dollars, materialization of that project would have to be realized by international monetary help. The national resource of geothermal energy is estimated at 230-860 MW and Lac Assal’s wind-power potential is estimated at 100 MW.

Figure 4, below, will give the reader a necessary understanding of the broad relationships amongst the most significant terrain features, some of which are (such as the glaring white salt flats northwest of Lac Assal) almost vegetation-less. The near sterility of the arid desert landscape is clear (Fig. 4).



Figure 4. Lac Assal and its salt flat—so tantalizingly close to the global ocean! *Image source:* http://commons.wikimedia.org/wiki/Atlas_of_Djibouti.

A greening of this East African ecosystem-country could serve as an inspiration to many peoples living in similar landscapes to research and develop the sub-surface geothermal energy resources via the technologies we present in this article.

CANALS AND DOMES

Not long after Lac Assal was first mapped topographically, macro-engineering proposals were made public that an 12 km-long canal, excavated through the land barrier between the inland, permanent body of syrupy brine 155 m below global sea-level and the Gulf of Tadjoura, would permit the massive generation of hydropower locally. (A gravity-fed canal must be used because 10 m is the maximum for seawater transfer by siphon.) Inflowing seawater from the Gulf of Aden would, of course, mix with Lac Assal's gushing geothermal spring water where the stagnant water's temperature is 80-100⁰ C during the daytime and nighttime. Pierre Gandillon (1931) proposed a canal-enabled hydro-solar facility in the Republic of Djibouti and he was followed by George A. Whetstone (1954), L. Le Grain (1955) and, finally, by El Sayed M. Hassan (1961). Significantly, long-distance international electricity transmission lines were an unconsidered option by these famously imaginative hydrological and hydrogeological investigators.

Macro-engineers have proposed city-covering inflatable (and geodesic) domes. Buckminster Fuller, in the 1960s, suggested a hemispherical geodesic dome 3 km-wide and 1.6 km-tall could enclose a part of New York City (USA) from the East River to the Hudson River at 42nd Street, and, north and south, from 62nd Street to 22nd Street. His dome, composed of wire-reinforced, one-way transparency, shatter-proof glass mist-plated with fine particles of aluminum to reduce internal solar glare whilst admitting sunlight would mass at 4,000 tonnes and cost ~200 million 1960 US dollars; adjusting for inflation since 1960, the *circa* 2009 cost would be ~1.433 billion dollars!

On 8 December 1992, Robin Berg and Timothy Berg were awarded a US Patent, #5168676, for their "Horizontally Ribbed Dome for Habitation Enclosure". The Bergs imagined "...domes having a minimum radius of one-half mile [~0.804 km]" composed of graphite-reinforced composite trusses and panels of clear plastic. Alexander A. Bolonkin and R.B. Cathcart (2007) have described huge inhabitable domes for use in the Arctic and in Antarctica. We assert here that a single dome or a series of small interconnected domes could cover Lac Assal and its adjacent bedded sea-salt terrain, approximately 115 km², with the macro-engineering aim of creating a huge distillation installation!

The key positive impacts of our LAFDED (the "Lac Assal Freshwater Distillatory and Energy District") in the East African Republic of Djibouti are:

- (1) help create useful jobs and gainful employment
- (2) increase export potential (made freshwater, generated electricity)
- (3) improve the national standard of living and boost the nation's GDP
- (4) services and infrastructure nationwide will be enhanced
- (5) provide a new and unique tourist industry attraction
- (6) cause the implementation of new Green landscape management measures

Some of the key negative impacts of LAFDED are:

- (1) permanent loss of open and unblemished desert landscape to seawater flooding and new buildings
- (2) some incidental decrease in aesthetic value of the distinctive salt flats and Lac Assal
- (3) land vehicle movements of automobiles and trucks on newly-paved highways will induce smog in the air and cause additional road accidents
- (4) new unplanned human settlements (spontaneous village type) may spring up
- (5) seaport development, and the attendant increase in oceanic-shipping arrivals and departures, will cause some offshore damage to the seafloor and seawater in the Gulf of Tadjoura and even the Gulf of Aden

Nevertheless, we propose a new kind of freshwater distillation and geothermal energy tower in the next section of this article.

GEOTHERMAL RESOURCES

Most of Africa's geothermal resources are located in its Rift Valley, one of the geologic wonders of the world. The Rift Valley spans roughly 6,000 kilometers across East Africa and runs through Kenya, Ethiopia, Djibouti a. s. o. (Poole, 2010). Kenya and Djibouti have the highest potentials for geothermal resources in East Africa. The technically exploitable geothermal potential in the different Djiboutian regions is currently estimated to range between 350 and 650 MW. The economically exploitable capacity for the Lac Assal-Ghoubbet region only is >100 MW; that is much more than the current requirements of Djibouti. The studies done on the territory showed that there are two kinds of reservoirs; a deeper one (over 2,000 m depth with >350°C) and a super-incumbent zone (between 300 m and 600 m with a 200°C resource). Other estimates are ten times more optimistic and range from 2,000 MWe (megawatts electric) to 7,000 MWe. This unmistakably shows that further investigations of the potential are required. Lately, there has been keen interest by many American investors, especially in infrastructure projects. Kenya was one of the first African states to develop its geothermal energy potential. The KenGen (Kenya Electricity Generating Company) has built three plants—Olkaria I (45 MW), Olkaria II (65 MW), and Olkaria III (48 MW)—with its American investing partner company Ormat Technologies, located in Nevada, USA. Among the companies competing for geothermal resources in other parts of the Rift Valley are Mitsubishi Heavy Industries, a global manufacturer of power equipment, and Reykjavik Energy (REI), which has developed geothermal energy macro-projects in Iceland.

So far, only about 200 MW of geothermal power have been installed in Kenya and 4 MW in Ethiopia. In Djibouti, research had been going on for the last 30 years. Exploratory wells have been drilled that strongly imply the presence of an exploitable geothermal resource. A TAA funded project on Djibouti geothermal exploration study was financed and completed between 1986 and 1992. However, no utilization has been commissioned yet. In Ethiopia, the R&D history is similar, but 4 MW are already installed. Reykjavik Energy is currently implementing a contract with the Government of Djibouti for a 50 MW geothermal power plant in the Lac Assal Area, about 100 km west of Djibouti City. Djibouti currently derives all its electricity from diesel generators, so power from geothermal plants in this country is intended for the general market. There are also large naval bases in Djibouti that generate their own electricity that are potential customers. There are also some other prospects for the development of Djibouti geothermal resources (Chideh, 2006). As part of the Lac Assal Project, REI intended geothermal power-plant is estimated to start production in 2012. The plant will supply Djibouti with Green electricity, replacing its costly current diesel-generated electricity supply.

The regions of Assal, Dikhil, Obock and Arta are quite rich areas and could enable the production of geothermal power fluid-direct use. The promising region of Lac Assal can, early on, supply a first increment of 30 MW; the studies completed in the Obock region showed that there is a possibility to project in a short term, the creation of a pilot geothermal central plant producing 5 MW. In a 2008 study, carried to conclusion by a team from Iceland in the Fiale region of Lac Assal is considered the most promising, with favorable geological setting, including a 3-4 km² reservoir with temperatures >240 °C. As the reader shall soon see, this working fluid temperature is ideal for driving the gravitational draught tower of a complex power plant with cold air turbine.

THE LAFDED GEOTHERMAL GRAVITY DRAUGHT POWER-PLANT

It is a demonstrated fact that the most efficient means to transform heat, namely enthalpy, into mechanical work is derived by adding a gravitational acceleration of the hot air by thermal draught in the gas-dynamical chain (Günter 1931, Unger 1988, Rugescu 2005). The source of heating was first considered as by the solar energy, although any type of heater may be considered (geothermal, nuclear, biofuel). The possibility to efficiently extract work from a geothermal resource of heat through a gravitational draught amplification was previously suggested (Rugescu and Tsahalis, 2007). The block-diagram of the draught tower in Figure 5 is considered for modeling its working efficiency in the LAFDED scheme. The air intake with the laminator device is the first element of the gas-dynamical chain, followed by the one-stage air turbine of Zoelly type (the continuous cascade of accelerating vanes plus the turbine rotor), the air heater and the air column within the tall part of the tower at last. An unrestricted upper opening for atmospheric release is closing the circuit. In order to exploit the geothermal heat resource, the heating scheme is different from the solar tower concept. In the present macro-project, the solar receiver is replaced by the geothermal water-air heat exchanger. Otherwise the working principle of the draught tower is identical. From the macro-engineering point of view, the removal of the solar array of heliostats considerably reduces the necessary land surface and the problem of mirror system maintenance. The geothermal version of GIGANT is called LAFDED and

Under these assumptions, the efficiency of the gravitational draught in the tower was already thoroughly investigated (Unger 1988, Rugescu 2005), without the involvement of the turbine however. A minute unsteady characterization of the turbine tower has already been developed (Cirligeanu et al., 2010). A simplified and fast assessment method of the tower efficiency is considered in the following.

Into the simplified 1-D computing scheme the main stages of the tower with turbine, corresponding to the set-up scheme from figure 1-a, are nominated in Figure 7.

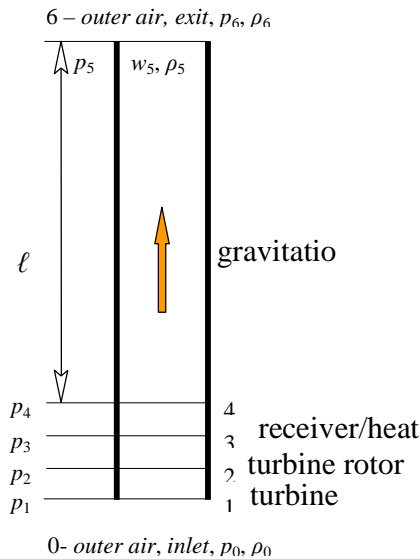


Figure 7: Main stations of the GIGANT draught tower model (Rugescu et al., 2005).

It succeeds in imparting a near sonic velocity c_2 to the airflow at rotor entrance “2”. The rotor of Zölly turbines is of equal pressure type and consequently the magnitude of the blade angle $|\beta|$ at entrance and exit is the same (equal angles rotor), while their sign is opposite. This forces the magnitude of the relative velocity inside the blades’ channel to preserve constant magnitude at a given instant, still opposite relative to the axis. A continuous turn of the airflow occurs into the channel. As a result, the high absolute velocity c_2 at rotor entrance reduces to the value and direction of the axial velocity c_{3a} at rotor exit (Figure 7, $c_3 \equiv c_{3a}$). This way the kinetic energy is sharply reduced by transfer of the equal amount of work to the turbine shaft, which means to the consumer (electric generator) from outside. From the mass continuity condition the axial speed c_{3a} can never be zeroed and it remains as a small, intrinsic and unavoidable loss of power into the gravity accelerator. All the other thermal parameters preserve constant along the rotor. To reduce pressure and friction losses to a minimum, the position angle of the blades at entrance is set equal to the nominal β value and the things are going that well for the nominal flow and rotational rate.

At non-equilibrium the air enters the blades under different angles, producing a lot of turbulence, friction losses and a reduction in the absolute velocity c_1 . At turbine start for example, due to the blunt turn of the speed from the direction of c_1 to the direction of w_1 a lower kinetic energy is delivered to the shaft. As the rotor gains speed this difference is gradually diminishing and finally ends into the steady-state condition described above. The model of the turbine that describes this start-up transient behavior simply reads

$$J_s \frac{d\omega}{dt} = M_N (1 - \bar{\omega}) \quad (1)$$

where J_s is the moment of inertia of the entire rotating shaft, M_N the nominal driving couple, ω_N is the nominal circular frequency and $\bar{\omega} = \omega / \omega_N$ is the relative circular frequency.

For the simplest case when the driving couple is given as constant, the angular acceleration $\varepsilon = d\omega / dt$ becomes a linear function of the circular frequency lag, ceasing at the nominal rate. Although simplifying, this case is useful to estimate the time constant T_N of the turbine shaft itself. The equation of motion (1) is re-written as

$$J_s \frac{d\omega}{dt} = M_N - m_N \omega \quad (2)$$

with $m_N = M_N / \omega_N$. It manifests the solution

$$\omega = \omega_N \left(1 - e^{-\frac{m_N t}{J_s}} \right) \equiv \omega_N \left(1 - e^{-\frac{t}{T_N}} \right). \quad (3)$$

Consequently, the linear rotor presents a time constant given by

$$T_N = \frac{\omega_N \cdot J_s}{M_N}. \quad (4)$$

The estimate for the moment of inertia of the STRAND shaft gives $J_s \cong 200 \text{ kg}\cdot\text{m}^2$ and this ends in $T \cong 2 \text{ s}$, which means the same order of magnitude with the airflow itself. It is observed in these computations that the nominal power output relates the shaft couple and the frequency by

$$P_N = M_N \cdot \omega_N.$$

In fact the unsteady motion is not that simple, and the driving moment must be computed at each moment from the equation of impulse, with \bar{r} for the mean value of the radius within the rotor, as

$$M_N = 2 \cdot \rho_2 A \cdot \bar{r} c_{2a} (c_{2t} - \bar{r} \omega). \quad (5)$$

From this parabolic dependence, it is found again the known fact that the power output goes through a maximum ($\partial P_N / \partial (\bar{r} \omega) = 0$) for

$$\bar{r} \cdot \omega_N = \frac{c_{2t}}{2}$$

from where the optimal turning rate and size of the turbine are derived. In these relations the magnitude and inclination of the absolute velocity of the air at stator exit c_2 is a given parameter that depends upon the optimal level allowed by the entire tower under its best working conditions.

These relations are not directly involved in the computational scheme, because the significant sudden jump of the axial velocity through the turbine is of macro-engineering interest. When given by a steady thermal equation

$$\Delta c_{13} \equiv c_3 - c_1 = c_1 (A_1 \rho_1 / A_3 \rho_3 - 1), \quad (6)$$

it hides the transient regime of the start and other unsteady variations, that must be added through extra equations. The connection between the local velocity at rotor entrance c_2 and the rotating rate ω results, for example, from the triangle of speeds, where the direction β of the relative velocity \mathbf{w} is imposed by the geometry of the rotor blades, as drawn in Figure 8, below.

From the geometry of the triangle the relation results $c_2 \sin(\beta_2 - \alpha_2) = \bar{r} \omega \sin \beta_2$, or

$$c_2 \cos \alpha_2 - c_2 \sin \alpha_2 \cot \beta_2 = \bar{r} \omega. \quad (7)$$

The moment of the impulse must be introduced in order to show up the fast transient effects. The formula (5) will be used with consideration of (7) to write

$$J_s \frac{d\omega}{dt} = 2 A_1 \rho_1 c_1 \bar{r} c_2 \sin \alpha_2 \cot \beta_2 \cdot (1 - \bar{\omega}) \equiv 2 \bar{m} \bar{r} c_{2a} \cot \beta_2 \cdot (1 - \bar{\omega}). \quad (8)$$

At each moment the rotating rate reaches the value that satisfies this equation, while the local speed c_2 , its angle α_2 and the air density ρ_2 should result from the local conditions, considered an isentropic expansion.

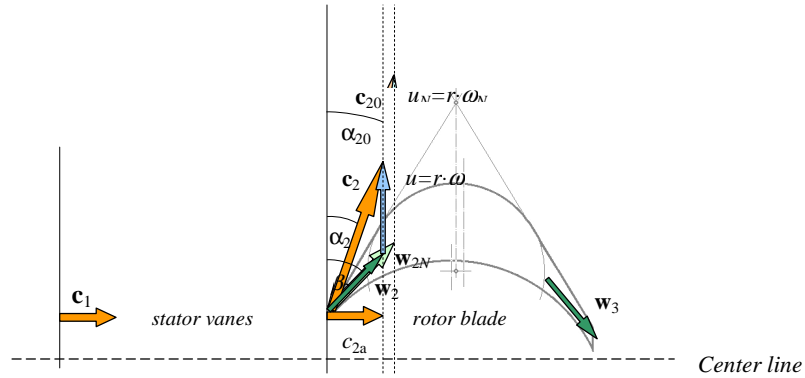


Figure 8. Modified rotor speed distribution at non-nominal flows.

This means that the re-compression at the governor exit does not involve shocks, or that they may be ignored. The losses should be considered through an experimental coefficient of efficiency. Then the local conditions are indicated by the set of equations

$$A_1 \rho_1 c_1 = A_2 \rho_2 c_2, \quad (\text{mass conservation}) \quad (9)$$

$$\frac{c_1^2}{\sin^2 \alpha_2} \left(\frac{\rho_1}{\rho_2} \right)^2 + L^2 \left(\frac{\rho_2}{\rho_1} \right)^{\kappa-1} = c_1^2 + L^2, \quad (\text{Bernoulli}) \quad (10)$$

where L denotes the maximal (limiting) speed of the air through the isentropic expansion,

$$L^2 \equiv \frac{2\kappa}{\kappa-1} R_1 T_1.$$

It manifests as if the speed at stator exit were lower than the one in steady expansion, up to the value c_2 , limited by the circular frequency ω and blades' direction β through the triangle relation (7). Note: the unsteady value for the velocity inclination α_2 is greater than the nominal value α_{2N} and should result from the set of four equations (7)-(10). They are complete for determining the four unknowns of the macro-problem. As a direct check, for a virtual case with no deviation of the velocity within the governor ($\alpha_2 = \pi/2$), $\sin \alpha_2 = 1$ and the Bernoulli equation (10) shows that no expansion takes place into the stator ($\rho_1/\rho_2 = 1$), consequently no energy release into the rotor could occur.

For convenience, in the computational scheme the circular frequency ω is replaced by the local speed c_2 . The time dependent values of the parameters stand for the conditions at tower entrance ($x=0$) in the numerical scheme described in (Cirligeanu et al., 2010).

THE GEOTHERMAL GRAVITY DRAUGHT EFFICIENCY FOR LAFDED

Grounded on the above mentioned computational scheme the geothermal power plant has an optimal efficiency when the heating of the draught air comes to around 200°C (Figure 9), which means a complete fit with the geothermal condition around Lac Assal, Djibouti. To derive the efficiency the basic equation of motion of the air within the tower becomes (Rugescu, 2005)

$$\frac{\Delta p(\ell)}{g \rho_0 \ell} \equiv \frac{1+r-k}{1-r} \cdot \frac{\dot{m}^2}{2g \ell \rho_0^2 A^2} + \frac{\Delta p_f(\ell)}{g \rho_0 \ell} - r = 0. \quad (11)$$

For small values of the friction loss the equilibrium mass flow rate becomes

$$\frac{\dot{m}^2}{2g\ell\rho_0^2A^2} = \frac{r(1-r)}{1+r-k}, \quad (12)$$

or slightly greater only than the value in the previous limit model (Unger, 1988).

When the friction losses are considered, the accurate value for the quadratic mass flow rate results from the second degree equation (11),

$$a\left(\frac{\dot{m}}{\dot{m}_\ell}\right)^2 + b\frac{\dot{m}}{\dot{m}_\ell} - r = 0, \quad (13)$$

where at the nominator a reference free-fall mass flow rate appears,

$$\dot{m}_\ell = w_\ell \rho_0 A,$$

based on the Torricelli free-fall velocity $w_\ell^2 = 2g\ell$ and the constants are

$$a = \frac{r/R}{w_\ell^2 \rho_0^2 A^2}, \quad b = \frac{32 v_0}{AD^2 g \rho_0} \left(\frac{T_w}{T_c}\right)^{1.7}. \quad (14)$$

or a slim, tall stack of $\ell/D = 70/2$ the contribution of friction is very small,

$$b/a = 2\%,$$

surely indicating that the actual difference between the non-friction flow and the real flow is smaller than ~0.05%. Consequently the non-friction result in (12) should be considered accurate enough. Its quadratic form shows the known fact that the heating of the inner air presents an optimal value and there exist an upper limit of the heating where the flow stack ceases. From the formula (12) it results that the non-dimensional quadratic mass flow rate R^2 is in fact the squared ratio of the exhibited stack entrance speed w_1 over the free-fall speed w_ℓ , due to constant cross-section area of the stack,

$$R^2(r) \equiv \left(\frac{w_1}{w_\ell}\right)^2 = \frac{r(1-r)}{1+r-k}, \quad R^2(r) \equiv \frac{\dot{m}^2}{w_\ell^2 \rho_0^2 A^2} = \frac{r(1-r)}{1+r-k}. \quad (15)$$

The entrance speed exhibits a maximum at the theoretically optimal heating r_{opt} ,

$$dR^2/dr = 0, \quad r_{opt}^2 + 2(1-k)r_{opt} - (1-k) = 0, \quad (16)$$

$$r_{opt} = -(1-k) + \sqrt{(1-k)(2-k)}.$$

The optimal heating for the standard air appears at a relative density reduction

$$r_{opt} \equiv (\rho_0 - \rho)/\rho_0 = 0.392033,$$

meaning an equal increase of the absolute temperature of $(1+r)$ times, when the normal air temperature should be raised with around 200°C above 27°C to achieve a maximal discharge, independent of the stack geometry. These values are an optimal response to the craft balance between the drag of the inflated hot air and its buoyant force, due to Archimedes' effect (Unger, 1988).

The behavior of the chimney flow for various heating intensities of the airflow, in the limit case of equal far stagnation pressures (FSP), is reproduced in Figure 9. The denoted curve is the other limiting case of equal static pressures (ESP) at the chimney's exit rim.

The free mass flow rate in formula (12) presents two roots where the flow ceases, at its origin $r = 0$ and at a maximal limit $r = 1$. These can not and do not hang on the exit assumptions, while the optimum heating point

does. Stack permeability is slightly higher for FSP. The above integral theory, thus, also allows for assessing the velocity increase at the tube entrance w_1 .

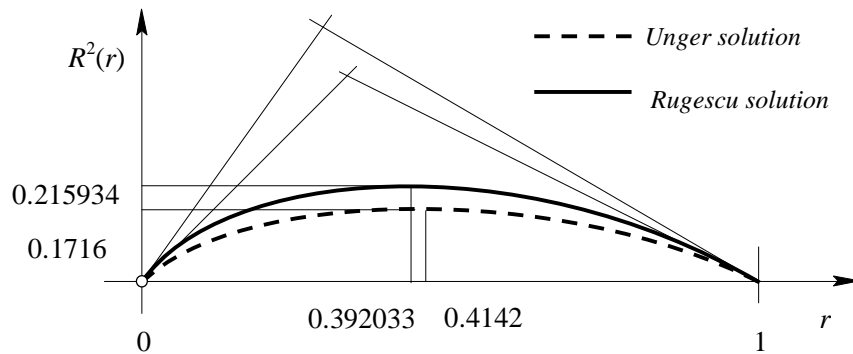


Figure 9. Stack discharge R^2 versus air heating intensity r .

The maximal value of the speed in the zone 1 from above is

$$w_{1\max} = R_{\max} \cdot w_\ell, \quad (17)$$

depending on the tower's height through the Torricelli speed w_ℓ . For the same example of a 70m tall tower the maximal constant area velocity of the entering air is roughly

$$w_{1\max} \sqrt{2g\ell \cdot R_{\max}^2} = \sqrt{1372.931 \cdot 0.2159} = 17.2 \text{ m/s.}$$

After the heating the velocity should increase $(1+r)$ times, to the otherwise moderate value of $w_2 = 20.9 \text{ m/s.}$, denoting very low air turbulence, if any at all.

The accelerating potential in a largely contracted nozzle goes in this case to more than 20 times the w_1 value, namely to the considerable boost of 340 m/s. Taller towers may contribute to further improvement of this potential. The rarefaction of the airflow in the nozzle, combined with its limited diameter, shows that such an aerodynamic rig is turned to small values of the Reynolds number rather, but this is the very realm where the aero-acoustics of noise generation is significant. We have no desire whatsoever to create a noise pollution macro-problem in the small ecosystem-state of Djibouti!

Both numerical simulations of ducted airflow and experimental measurements on a scale model were called in support of the above estimations.

CONCLUSION

The efficiency of the Lac Assal Freshwater Distillatory and Energy District's proposed gravity draught power-plant is quite obvious, and when coupled with existing supplies of naturally-heated saline hot water from local underground geothermal resources, it represents a very powerful means of providing electricity in remote regions like, typically, the Republic of Djibouti's Lac Assal region. The capacity of the power-plant is great enough to

simultaneously secure seawater desalination and, subsequently, a reliable civilian freshwater supply over a large section of the ecosystem-nation. Our estimates show that an urban habitat of ~10,000 people may be served by a medium-size, draught power-plant, like the one considered in detail above. The application of that macro-project solution to the Lac Assal region, in the form of our proposed LAFDED seems especially useful.

REFERENCES

***, The Djibouti Geothermal Project, 2008.

Backer, H., Clin, M and Lange, K (1973) Tectonics in the Gulf of Tadjura. *Marine Geology* 15: 309-327.

Bolonkin, AA and Cathcart, RB (2007) Inflatable 'Evergreen' dome settlements for Earth's Polar Regions. *Clean Technologies and Environmental Policy* 9: 125-132.

Brisou, J, Courtois, D. and Denis, F (1974) Microbiological Study of a Hypersaline Lake in French Somaliland. *Applied Microbiology* 27: 819-822.

Cathcart, R.B. and Badescu, V. (2004) Architectural Ecology: A Tentative Sahara Restoration. *Int. J. of Environmental Studies* 61: 145-161.

Cathcart, R.B. (2008) Kra Canal (Thailand) excavation by nuclear-powered dredges. *International Journal of Global Environmental Issues* 8: 248-255.

Chideh, A.F., Pilot Project for Energy and Mining Economic Beneficiation from Assal (Djibouti) Geothermal and Mineral Resources, Geothermal Resources Council GRC-2006 Annual Meeting, Tuesday, September 12.

Cirligeanu, R., Rugescu, R. D., Bogoi, A. (2010), TRANSIT code for turbine flows in solar-gravity draught power plants, Paper GT2010-22518, *Proceedings of the ASME International Conference on Gas Turbines*, June 14-18, 2010, Glasgow, Skotland, UK.

Gandillon, P (1931) Amenagement et mise en valeur de la cote Francaise des Somalie. *Memoires de la Societe des Ingenieurs Civils de France* 84: 967-977.

Gasse, F. and Fontes, J-C. (1989) Palaeoenvironments and Palaeohydrology of a Tropical Closed Lake (Lake Asal, Djibouti) Since 10,000 yr B.P. *Palaeogeography, Palaeoclimatology, Palaeoecology* 69: 67-102.

Günter, H., In hundert Jahren – Die künftige Energieversorgung der Welt, *Kosmos, Gesellschaft der Naturfreunde, Franckh'sche Verlagshandlung*, Stuttgart, 1931.

Hassan, ESM (1961) Power from the Sea. *Proc. Amer. Soc. Civil Engineers* 87: 21-27.

Le Grain, L (1955) Remarques au sujet de la centrale hydro-solaire de lac Assal: Autres possibilites d'utilisation de ce lac. *La Houille Blanche* 10: 207-210.

Mugnier, C.J. (2008) Grids and Datums: Republic of Djibouti. *Photogrammetric Engineering & Remote Sensing* 74: 1183-1185.

Poole, L., Jun 22, 2010, Geothermal Companies Vie for African Development Contracts, renewableenergyworld.com.

Rowland, J.V., Baker, E., Ebinger, C.J., Keir, D., Kidane, T., Briggs, J., Hayward, N. and Wright, T.J. (2007) Fault growth at a nascent slow-spreading ridge: 2005 Dabbahu rifting episode, Afar. *Geophys. J. Int.* 171: 1226-1246.

Rugescu R. D., *Thermische Turbomaschinen*, ISBN 973-30-1846-5, Ed. D. P. Bucharest, Ch.7, 2005.

Rugescu, R. D., Demos T. Tsalhalis, "Improved unsteady approach to gravity draught power plants", *Proceedings of the International Workshop on Acoustics and Vibration-IWAVE2007*, Cairo, Egypt, September 8-9, 2007

Rugescu, R. D., Chatcat, R., Rugescu, D. R., Electricity and Freshwater Macro-project in the Arid African Landscape of Lac Assal, Eighth International Conference on Structural Dynamics, EURO-DYN-2011, Leuven, Belgium, 4-6 July 2011.

Schuiling, R.D., Badescu, V, Cathcart, R.B., Soud, J. and Hanekamp, J.C. (2007) Power from closing the Red Sea: economic and ecological costs and benefits following the isolation of the Red Sea. *Int. J. Global Environmental Issues* 7: 341-361.

Strahan, D. (2009) Green Grid. *New Scientist* 201: 42-45.

Unger, J., *Konvektionsströmungen*, B. G. Teubner, ISBN 3-519-03033-0, Stuttgart, 1988.

Vigny, C., de Chabaliere, J-B, ruegg, J-C, Huchon, P., Feigle, K.L., Cattin, R., Asfaw, L. and Kanbari, K. (2007) Twenty-five years of geodetic measurements along the Tadjoura-Asal rift system, Djibouti, East Africa. *Journal of Geophysical Research* 112: B06410.

Whetstone, GA (1954) *La Houille d'Or*. *Water Power* 6: 272-274.